Theory and Experiment of a Rectangular Slot on a Sphere

Kwok Wa Leung, *Member, IEEE*

***Abstract*— A rectangular slot on a spherical cavity is studied theoretically and experimentally. The Green's functions interior and exterior to the cavity are found rigorously using the mode-matching method. An integral equation of magnetic current in the slot is formulated, which is solved using the moment method. The singularity problem in admittance calculations is tackled and the result is very computationally efficient. Both the slot and cavity resonances are examined. Moreover, the natural and forced resonances of the cavity are addressed. The effects of slot length, cavity size, excitation location, and cavity dielectric constant on the input impedance are discussed. Very good agreement between theory and experiment is obtained.**

***Index Terms*— Modal analysis, moment method, resonance, spherical cavity.**

I. Introduction

AN AZIMUTHAL or zonal slot cut on a conducting sphere has been studied extensively [1]–[6]. However, only little attention was received for the rectangular slot. Such a structure is inherently an interesting problem and can be used as a gain standard [2]. Furthermore, the rectangular slot offers a higher flexibility than the azimuthal slot in designing a spherical array, which can be used to avoid the scanning problem of a planar array at low elevation. Thus far, studies of the rectangular slot on a sphere have only concentrated on the radiation pattern [2], scattering [7], [8], and mutual coupling [9]. Little or no information of the input impedance was found in the literature. In this paper, the input impedance of a rectangular slot cut on a conducting spherical cavity is studied theoretically and experimentally. Although the slot is not cavity-backed, the extension of the present theory to include the slot backing for practical applications is straightforward. Like the planar case [10], the slot can be excited by a microstrip feedline inside the sphere to admit a monolithic-microwave integrated-circuit (MMIC) integration, and the present theory can be easily extended to analyze the modified or other related structures. Moreover, the result can be useful as a means of testing approximate theoretical methods.

In this paper, the mode-matching method [11] is used to derive the Green's functions of the structure rigorously. An integral equation of the unknown magnetic current in the slot is formulated by matching the boundary conditions [12], [13], and the unknown current is solved using the moment method. To enhance the numerical computation, the modal Green's functions are presented as a sum of particular and homogenous solutions [11]. This allows a special treatment for the slowly convergent particular solutions. Although the homogeneous solutions themselves do not converge on the spherical boundary, it was found that their impedance integrals converge very quickly by using only a small number of modal terms. For the particular solutions, the technique of [14] is used to obtain a new result for a curvilinear slot. The integrals are expressed in forms analogous to the Richmond form so that they can be calculated in a straightforward manner. These make calculations of the input impedance very easy and fast.

Two kinds of resonance are found for the structure and are examined in this paper: the slot and cavity resonance. In particular, the natural and forced resonances of the cavity are addressed and discussed. The effects of slot length, cavity size, excitation location, and cavity dielectric constant on the input impedance are discussed. Measurements are done to check the calculations, and very good agreement between theory and experiment is obtained.

II. Formulation

The geometry of the structure is shown in Fig. 1, where a slot of length L and of width W is cut from a conducting spherical cavity filled with material of dielectric constant ε_r and of wavenumber $k_c = \sqrt{\varepsilon_r} k_0$. The center of the slot lies on the x-axis, and the slot subtends an angle from $-\phi_1$ to ϕ_1. In the following formulation, the fields are assumed to vary harmonically as $e^{j\omega t}$, which is suppressed. Moreover, $\vec{r}(r, \theta, \phi)$ and $\vec{r}'(r', \theta', \phi')$ refer to the field and source points, respectively. The superscripts or subscripts c and e are used to denote the interior and exterior regions of the cavity, respectively. It is assumed that the cavity is surrounded by air and $k_e = k_0$. From the equivalence principle, the slot can be shorted and the exterior and interior fields are now generated by the equivalent magnetic currents M_ϕ and $-M_\phi$, respectively. The equivalent configuration is shown in Fig. 2. For the ease of computation, the Green's functions are divided into their particular and homogeneous parts. The former represents radiation of a source in an unbounded medium, while the latter accounts for the boundary discontinuity. Following the procedure of [11], the interior and exterior Green's functions of H_ϕ are obtained. On the slot surface, we have $r = r' = a$, and the Green's functions are given by

$$G^{e,c} = G_P^{e,c} + G_H^{e,c} \tag{1}$$

Manuscript received February 3, 1998; revised June 15, 1998. This work was supported under the RGC Earmarked Research Grant 9 040 209.

The author is with the Department of Electronic Engineering, City University of Hong Kong, Kowloon, Hong Kong.

Publisher Item Identifier S 0018-9480(98)09053-X.

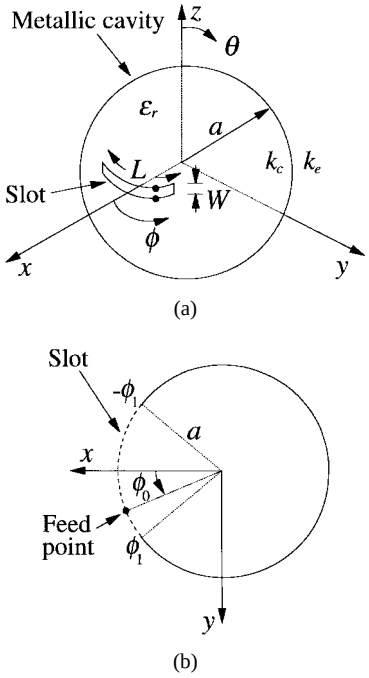

Fig. 1. Geometry of a slot on a sphere. (a) Perspective view. (b) Top view.

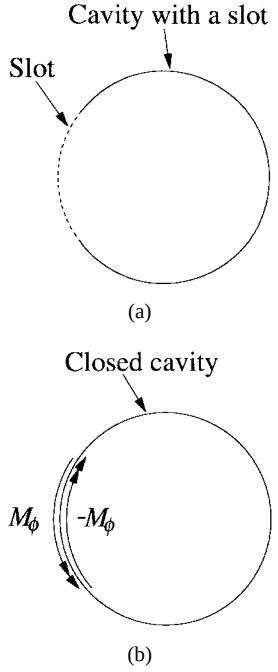

Fig. 2. The use of equivalence principle. (a) Original problem. (b) Equivalent problem.

where

$$G_P^{e,c} = \frac{-1}{4\pi a^2 \eta_{e,c}} \sum_{n=1}^{\infty} \frac{2n+1}{n(n+1)} \cdot \frac{\partial^2 P_n(\cos\xi)}{\partial\theta\partial\theta'} \cdot \hat{J}_n(k_{e,c}a)\hat{H}_n^{(2)}(k_{e,c}a) - \frac{1}{4\pi a^2\eta_{e,c}} \cdot \frac{1}{\sin\theta\sin\theta'} \cdot \sum_{n=1}^{\infty} \frac{2n+1}{n(n+1)} \frac{\partial^2 P_n(\cos\xi)}{\partial\phi\partial\phi'} \hat{J}_n'(k_{e,c}a)\hat{H}_n^{(2)'}(k_{e,c}a) \tag{2}$$

$$G_H^e = \frac{-1}{4\pi a^2\eta_e} \sum_{n=1}^{\infty} \beta_n^{\mathrm{TM}} \frac{2n+1}{n(n+1)} \frac{\partial^2 P_n(\cos\xi)}{\partial\theta\partial\theta'} \cdot \left[\hat{H}_n^{(2)}(k_e a)\right]^2 - \frac{1}{4\pi a^2\eta_e} \cdot \frac{1}{\sin\theta\sin\theta'} \sum_{n=1}^{\infty} \beta_n^{\mathrm{TE}} \cdot \frac{2n+1}{n(n+1)} \frac{\partial^2 P_n(\cos\xi)}{\partial\phi\partial\phi'} \left[\hat{H}_n^{(2)'}(k_e a)\right]^2 \tag{3}$$

$$G_H^c = \frac{-1}{4\pi a^2\eta_c} \sum_{n=1}^{\infty} \alpha_n^{\mathrm{TM}} \frac{2n+1}{n(n+1)} \cdot \frac{\partial^2 P_n(\cos\xi)}{\partial\theta\partial\theta'} \cdot \left[\hat{J}_n(k_c a)\right]^2 - \frac{1}{4\pi a^2\eta_c} \cdot \frac{1}{\sin\theta\sin\theta'} \sum_{n=1}^{\infty} \alpha_n^{\mathrm{TE}} \cdot \frac{2n+1}{n(n+1)} \frac{\partial^2 P_n(\cos\xi)}{\partial\phi\partial\phi'} \left[\hat{J}_n'(k_c a)\right]^2 \tag{4}$$

$$\cos\xi = \cos\theta\cos\theta' + \sin\theta\sin\theta'\cos(\phi-\phi') \tag{5}$$

$$\alpha_n^{\mathrm{TE}} = -\hat{H}_n^{(2)}(k_c a)/\hat{J}_n(k_c a) \tag{6}$$

$$\alpha_n^{\mathrm{TM}} = -\hat{H}_n^{(2)'}(k_c a)/\hat{J}_n'(k_c a) \tag{7}$$

$$\beta_n^{\mathrm{TE}} = -\hat{J}_n(k_e a)/\hat{H}_n^{(2)}(k_e a) \tag{8}$$

$$\beta_n^{\mathrm{TM}} = -\hat{J}_n'(k_e a)/\hat{H}_n^{(2)'}(k_e a) \tag{9}$$

and $\eta_{e,c}$ denote the wave impedances. Observe that the Green's functions $G^{e,c}$ are reciprocal in $\vec{r}$ and $\vec{r}'$, which is to be expected. In (2)–(4), $P_n(x)$ is the Legendre polynomial of degree n, and $\hat{J}_n(x)$ and $\hat{H}_n^{(2)}(x)$ are the spherical Bessel function of the first kind and spherical Hankel function of the second kind, respectively. Both of them are of order n and of Schelkunoff type [15, p. 268]. All other symbols have the usual meanings. It should be mentioned that as the particular solutions are solved under the free-space condition, (2) is common to both the interior and exterior regions, except that each region has its own constitutive parameters. In (3) and (4), α_n^{TE}, α_n^{TM}, β_n^{TE}, and β_n^{TM} are reflection coefficients at the cavity boundary. It is interesting to note that when the denominators of α_n^{TE} and α_n^{TM} are set to zero, we obtain the characteristic equations for cavity resonances of TE and TM modes, respectively. The eigenvalues of the equations have been well studied elsewhere [15, pp. 269–271]. On the other hand, putting the denominators of β_n^{TE} and β_n^{TM} to zero gives the characteristic equations for complex scattering resonances of TE and TM modes, respectively. In deriving (2)–(4), the double summations in the modal expansion have been reduced to the single summations by using the addition theorem for Legendre polynomials

$$P_n(\cos\xi) = \sum_{m=0}^{n} \frac{2}{\Delta_m} \cdot \frac{(n-m)!}{(n+m)!} P_n^m(\cos\theta) P_n^m(\cos\theta') \cdot \cos m(\phi-\phi') \tag{10}$$

where $\Delta_m = 1$ for $m > 0$ and 2 for $m = 0$.

Let $\vec{J} = J_s\hat{\theta}$ be the excitation (electric) current density, then we have

$$H_\phi^e - H_\phi^c = J_s \tag{11}$$

from which the following integral equation for the magnetic current density M_ϕ is obtained:

$$\iint_{S_0} G^e\left(\vec{r},\vec{r}'\right)M_\phi(\phi')\,dS' - \iint_{S_0} G^c\left(\vec{r},\vec{r}'\right)[-M_\phi(\phi')]\,dS' = J_s \quad (12)$$

where S_0 is the slot surface. The delta gap source is used to model the excitation current and, therefore, $J_s = -(I_0/a)\delta(\phi-\phi_0)$, where I_0 and ϕ_0 are the current amplitude and ϕ coordinate at the feed point, respectively. Let $K_\phi(\phi) = M_\phi(\phi)W$ be the magnetic current, then (12) becomes

$$\frac{1}{W}\iint_{S_0}\left[G^e\left(\vec{r},\vec{r}'\right)+G^c\left(\vec{r},\vec{r}'\right)\right]K_\phi(\phi')\,dS' = \frac{-I_0}{a}\delta(\phi-\phi_0). \quad (13)$$

Using the moment method, the magnetic current is expanded in terms of unknown voltage coefficients V_n's as follows:

$$K_\phi(\phi) = \sum_{n=1}^{N} V_n f_n(\phi) \quad (14)$$

where $f_n(\phi)$'s are piecewise sinusoidal (PWS) basis functions given by

$$f_n(\phi) - \begin{cases} \dfrac{\sin k_e'(h-a|\phi-\phi_n|)}{\sin k_e' h}, & a|\phi-\phi_n|<h \\ 0, & a|\phi-\phi_n|\geq h \end{cases} \quad (15)$$

in which

$$h = \frac{L}{N+1} \quad (16)$$

$$\phi_n = \frac{1}{a}\left(\frac{-L}{2}+nh\right) \quad (17)$$

and $k_e' = \sqrt{(\varepsilon_r+1)/2}k_0$ is the effective wavenumber of the slot. Insertion of (14) into (13) yields

$$\frac{1}{W}\sum_{n=1}^{N} V_n \iint_{S_0}\left[G^e\left(\vec{r},\vec{r}'\right)+G^c\left(\vec{r},\vec{r}'\right)\right]f_n(\phi')\,dS' = \frac{-1}{a}\delta(\phi-\phi_0) \quad (18)$$

where I_0 has been set to unity for convenience. By using the Galerkin's procedure, the following matrix equation is obtained:

$$[Y_{mn}^e + Y_{mn}^c][V_n] = [f_m(\phi_0)] \quad (19)$$

where

$$Y_{mn}^{e,c} = \frac{-1}{W^2}\iint_{S_0}\iint_{S_0} f_m(\phi)G^{e,c}f_n(\phi')\,dS'\,dS. \quad (20)$$

After V_n's are found, the input impedance is easily calculated from $Z_{\text{in}} = \Sigma_{n=1}^{N} V_n f_n(\phi_0)$. In Section III, we will discuss a technique to calculate $Y_{mn}^{e,c}$ efficiently.

III. Efficient Computation of $Y_{mn}^{e,c}$

To calculate the admittance elements $Y_{mn}^{e,c}$ efficiently, we first divide $Y_{mn}^{e,c}$ into their particular and homogeneous parts as follows:

$$Y_{mn}^{e,c} = Y_{\text{mnP}}^{e,c} + Y_{\text{mnH}}^{e,c} \quad (21)$$

where

$$Y_{\text{mnP}}^{e,c} = \frac{-1}{W^2}\iint_{S_0}\iint_{S_0} f_m(\phi)G_P^{e,c}f_n(\phi')\,dS'\,dS \quad (22)$$

and

$$Y_{\text{mnH}}^{e,c} = \frac{-1}{W^2}\iint_{S_0}\iint_{S_0} f_m(\phi)G_H^{e,c}f_n(\phi')\,dS'\,dS. \quad (23)$$

Direct evaluation of the homogeneous parts $Y_{\text{mnH}}^{e,c}$ is possible since the integrals of $G_H^{e,c}$ converge in a small number of modal terms, and the truncated $G_H^{e,c}$ are slowly varying functions. To solve the problems arising from $G_P^{e,c}$, we use the physical argument technique [11], [14] to replace the modal form of $G_P^{e,c}$ by a simple form that requires no summation. We then use the concept of equivalent radius [14] so that the magnetic currents now flow on a (curvilinear) cylindrical surface instead of the curvilinear slot. It can then be shown that the admittances $Y_{\text{mnP}}^{e,c}$ are given by

$$Y_{\text{mnP}}^{e,c} = -\int_{-\phi_1}^{\phi_1}\int_{-\phi_1}^{\phi_1} f_m(\phi) \cdot\left\{\frac{1}{\eta_{e,c}^2}\cdot\frac{-j\eta_{e,c}}{4\pi}\left[k_{e,c}\cos(\phi-\phi') + \frac{1}{k_{e,c}a^2}\frac{\partial^2}{\partial\phi^2}\right]\frac{e^{-jk_{e,c}R}}{R}\right\} \cdot f_n(\phi')a^2\,d\phi'\,d\phi \quad (24)$$

where

$$r_1 = \frac{W}{4} \quad (25)$$

and

$$R = \sqrt{4a^2\sin^2[(\phi-\phi')/2]+r_1^2} \quad (26)$$

are the equivalent radius and approximate distance between the field and source points on the cylindrical surface, respectively. (The exact and more accurate expressions of the distance are given in the Appendix). In (24), the term $(-j\eta_{e,c}/4\pi)[\cdot](e^{-jk_{e,c}R}/R)$ represents the Green's function of E_ϕ due to a $\hat{\phi}$-directed electric point current in free space, whereas the factor of $(1/\eta_{e,c}^2)$ is used to transform the electric quantities to magnetic ones. Observe from (26) that $R \neq 0$ and, thus, the singularity has been avoided. After simplification and rearrangement, we obtain (27), shown at the bottom of the following page, which is analogous to the Richmond form of a cylindrical dipole [16]. By using (27), $Y_{\text{mnP}}^{e,c}$ can be calculated in a straightforward manner. Of course, care has to be taken in performing the numerical integration around $\phi=\phi'$, where the integrand has a very sharp (but finite) amplitude due to the factor of $1/R^5$.

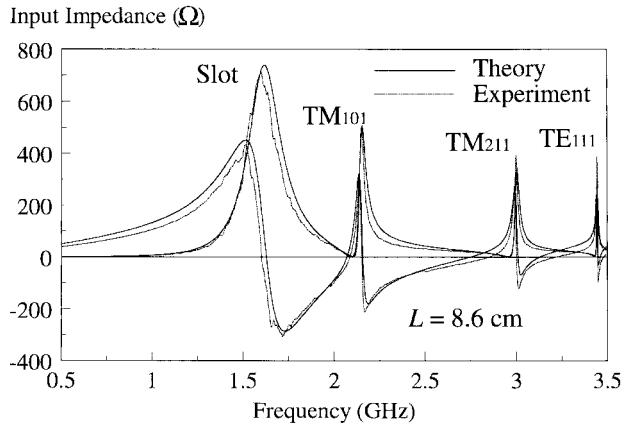

(a)

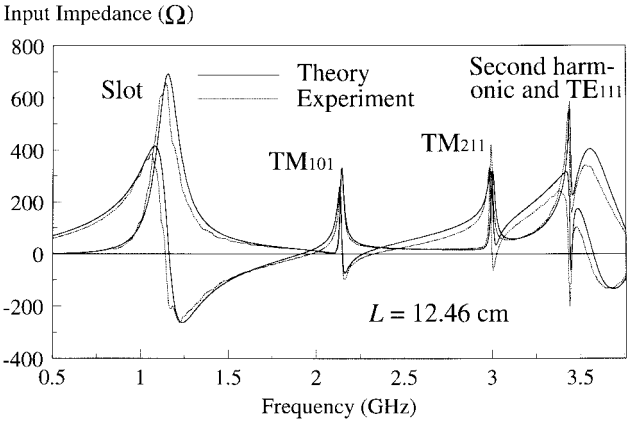

(b)

Fig. 3. Measured and calculated input impedance of the structure for different slot lengths: $a = 6.25$ cm, $W = 2.4$ mm, $\varepsilon_r = 1, \phi_0 = 0$. (a) $L = 8.60$ cm. (b) $L = 12.46$ cm.

IV. Measured and Calculated Results

To verify the theory, measurements were done using the image technique [17], [18]. Several hemispherical cavities of radius $a = 6.25$ cm were fabricated, whose edges were butted up against a 50×50 cm^2 copper image plane. Conducting adhesive tapes were used at the cavity edge to increase the conduction between the cavity and image plane. A coaxial probe of radius 0.62 mm was used to excite the half-slot of width $W/2$. The measurements were carried out using an HP8510C network analyzer, and the reference plane was set at the coaxial aperture using the port extension. The measured input impedances were multiplied by two to obtain the input impedance of the original configuration (a spherical cavity with a whole slot).

The input impedance of the structure for $L = 8.60$, 10.43, and 12.46 cm were measured and calculated, but only the results of $L = 8.6$ and 12.46 cm are shown in Fig. 3 for brevity. The convergence check of the moment method was done, and $N = 5$ was used in the following calculations. To obtain the converged impedance integrals of the homogeneous solutions, it was found that using about ten modal terms is sufficient for the first cavity resonance (TM_{101} mode) and 30 for the third resonance (TE_{111} mode). In this paper, 30 modal terms were used for $a = 6.25$ cm and fewer terms for a smaller cavity. With reference to Fig. 3(a) and (b), very good agreement between theory and experiment is obtained. Several resonances are found which are labeled in the figures. Note that the degenerate TM_{111}, TM_{201}, TM_{221}, and TE_{101} modes cannot be excited since the slot is bisected by the x–y plane. The first resonance is due to the slot, whose resonant frequency decreases with increasing slot length, as expected. Note that the slot length affects the impedance of the slot very slightly, as found in the planar case. Table I shows the measured and calculated resonant frequencies (zero reactance) of the slot for $L = 8.60$, 10.43, and 12.46 cm. With reference to Table I, the maximum error is 2.23%. For ease of comparison, the resonant frequencies predicted using the simple formula $f_r = c/(2L)$ are also shown in the table. As can be observed from Table I, the calculated value is always lower than the predicted value. Part of the reason is that the end effect of the slot, which effectively increases the slot length and thus decreases the resonant frequency, is not included in the simple formula.

TABLE I
Measured, Calculated, and Predicted Resonant Frequencies (Zero Reactance) of the Slot for $L = 8.6$, 10.43, and 12.46 cm. Other Parameters are the Same in Fig. 3

L (cm)	W (mm)	Measured (GHz)	Calculated (GHz)	error (%)	$f_r = c/(2L)$ (GHz)
8.60	2.4	1.60	1.63	1.88	1.74
10.43	2.8	1.34	1.37	2.23	1.44
12.46	2.4	1.14	1.16	1.75	1.20

For the cavity resonance, note that the fundamental mode is the TM_{101} mode, whereas it is the TE_{111} mode for a dielectric cavity of $\varepsilon_r \approx 10$ [11], [14]. It should be mentioned that the cavity resonances at zero reactance are caused by the slot, i.e., they are forced resonances. For the natural resonances, they occur at the points where the input resistance is minimum [18], [19]. This is because, at the natural resonances, the fields are distributed in a way that strongly resembles the closed cavity case. This forces the (tangential) E-field in the slot to vanish, causing the input resistance to be so small. Table II compares the calculated resonant frequencies of the natural resonances (minimum resistance) with those predicted using the eigenvalues for $L = 8.6$ cm. From Table II, it is seen that the predicted, calculated, and measured values are in excellent agreement. The measured and calculated forced resonant frequencies for $L = 8.6$ cm are given in Table III, where excellent agreement between theory and experiment is found (error <0.5%).

$$Y_{mnP}^{e,c} = \frac{-1}{\eta_{e,c}^2} \int_{-\phi_1}^{\phi_1} \int_{-\phi_1}^{\phi_1} f_m(\phi) \left\{ \frac{-j\eta_{e,c}}{4\pi} \cdot \frac{e^{-jk_{e,c}R}}{kR^5} \left[R^2(k_{e,c}^2R^2 - jk_{e,c}R - 1)\cos(\phi - \phi') - a^2(k_{e,c}^2R^2 - 3jk_{e,c}R - 3)\sin^2(\phi - \phi') \right] \right\} f_n(\phi') a^2 \, d\phi' \, d\phi \quad (27)$$

TABLE II
MEASURED, CALCULATED, AND PREDICTED NATURAL RESONANT FREQUENCIES OF THE CAVITY FOR $L = 8.6$ cm. OTHER PARAMETERS ARE THE SAME IN FIG. 3

Resonance mode	Cavity f_r (eigen value) (GHz)		Cavity f_r (min. resistance) (GHz)		
	k_0a	$f_r = c(k_0a)/(2\pi a)$	Calculated	Measured	error (%)
TM_{101}	2.744	2.10	2.10	2.10	0.0
TM_{211}	3.870	2.96	2.96	2.96	0.0
TE_{111}	4.493	3.43	3.43	3.43	0.0

TABLE III
MEASURED AND CALCULATED FORCED RESONANT FREQUENCIES OF THE CAVITY FOR $L = 8.6$ cm. OTHER PARAMETERS ARE THE SAME IN FIG. 3

Resonance mode	Measured (GHz)	Calculated (GHz)	error (%)
TM_{101}	2.15	2.16	0.47
TM_{211}	3.00	3.01	0.33
TE_{111}	3.45	3.45	0.00

Refer back to Fig. 3. As L increases, the resonant frequency of the second-harmonic slot resonance decreases and the influence of the harmonic upon the cavity TE_{111}-mode increases. (The first harmonic of the slot requires the magnetic current or the slot voltage to be zero at the center of the slot. Therefore, the first harmonic cannot be excited when the slot is center fed.) This can be seen from the fact that as L was increased from 8.6 to 10.43 cm, the minimum TE_{111}-mode resistance increased from a rather small value of 3.1 to 21.5 Ω. The interference between the second harmonic and the TE_{111} mode is obvious at $L = 12.46$ cm [see Fig. 3(b)]. Using $f_r = 1.5c/L$, the resonant frequency of the second harmonic for $L = 12.46$ cm is about 3.61 GHz. Since the actual resonant frequency is somewhat lower than this value due to the end effect, it is evident that the second-harmonic and TE_{111}-mode resonances are very close to each other. With reference to Fig. 3(b), as expected, the second harmonic and the cavity TE_{111} mode interfere with each other very strongly.

The resonant frequency of the slot has been lower than that of the TM_{101} mode. It is interesting to see what happens when the slot resonance has a higher frequency. For this purpose, an experiment using $L = 4.45$ cm was carried out. The estimated resonant frequency of the slot is about 3.3 GHz, which is higher than that of the TM_{101} mode (2.1 GHz). The measured and calculated results are shown in Fig. 4, where good agreement between theory and experiment is observed. With reference to Fig. 4, the TM_{101}-mode resonance now has a very sharp impedance, exhibiting a very high-Q characteristic. (The peak is too sharp to measure accurately.) At this resonance, the cavity has a very poor radiation loss and acts rather like a closed cavity. This shows that the influence of the slot upon the TM_{101} mode is small. Instead, as shown in Fig. 4, the slot now interacts strongly with the cavity TM_{211} mode.

Fig. 5 shows the calculated input resistance for $a = 4.0$, 5.0, and 6.25 cm, with $L = 10.43$ cm and $W = 2.8$ mm. For clarity, only the TM_{101} mode is shown for cavity resonance. With reference to the figure, the resonant frequency of the cavity is now significantly affected; as expected, the smaller

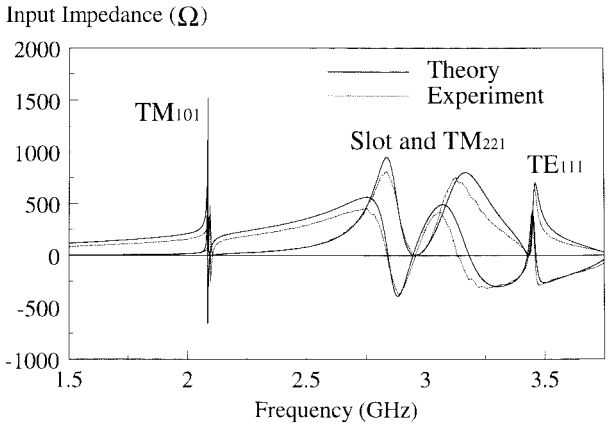

Fig. 4. Measured and calculated input impedance of the structure: $L = 4.45$ cm, $W = 2.4$ mm, $a = 6.25$ cm, $\varepsilon_r = 1$, $\phi_0 = 0$.

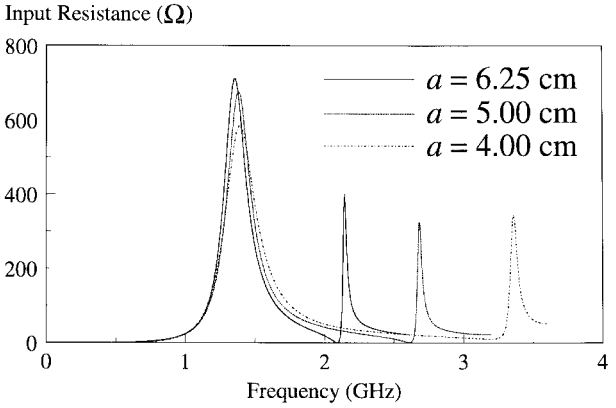

Fig. 5. Calculated input resistance of the structure for $a = 4.0$, 5.0, and 6.25 cm: $L = 10.43$ cm, $W = 2.8$ mm, $\varepsilon_r = 1$, $\phi_0 = 0$.

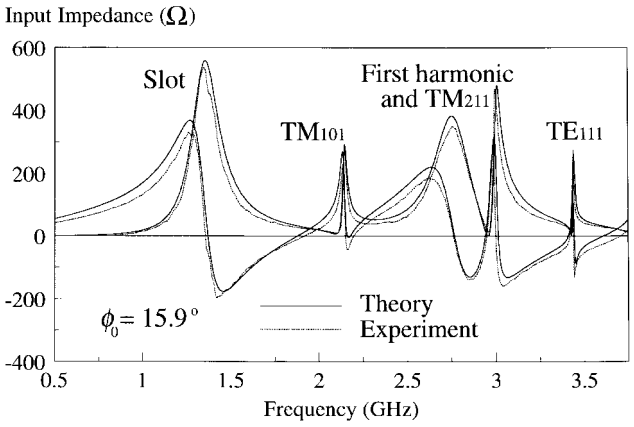

Fig. 6. Measured and calculated input impedance of the structure for an excitation offset $\phi_0 = 15.9°$: $L = 10.43$ cm, $W = 2.8$ mm, $a = 6.25$ cm, $\varepsilon_r = 1$.

the cavity, the higher the resonant frequency results. Observe that the resonant frequency of the slot is only slightly altered by the cavity size. From the figure, it is seen that using a smaller cavity leads to a smaller slot impedance. The results are similar to those of the cavity-backed slot antenna [18].

Fig. 6 shows the measured and calculated input impedances for an excitation offset $\phi_0 = 15.9°$ with $L = 10.43$ cm

and $W = 2.8$ mm. Good agreement between theory and experiment is obtained. With reference to the figure, the first harmonic of the slot, which has not been found previously for $\phi_0 = 0$, is now excited. The calculated resonant frequency of the first harmonic (zero reactance) is 2.76 GHz, which agrees excellently with the measured value. On the other hand, the predicted resonant frequency using $f_r = c/L$ is 2.88 GHz. In view of the end effect of the slot and the coupling of other resonances, the results are very consistent. The input impedance for $\phi_0 = 32.8°$ was also measured and calculated, and good agreement between theory and experiment was obtained. From the results of $\phi_0 = 0°$, $15.9°$, and $32.8°$, it was found that the input impedance at the fundamental slot resonance decreased as ϕ_0 increased. This is because, at the fundamental resonance, the slot voltage (magnetic current) is maximum at the center and decreases monotonically along the slot. A similar trend is also observed for the cavity TM_{101} mode. It was observed that at $\phi_0 = 32.8°$, the TM_{101}-mode reactance was shifted upward, significantly due to the influence of the strongly excited harmonic.

The input impedances for $\varepsilon_r = 3$ and 6 with $L = 10.43$ cm, $W = 2.8$ mm, $a = 6.25$ cm, and $\phi_0 = 0°$ were calculated. It was found that, as expected, the higher the dielectric constant, the lower the resonant frequency and the higher the Q-factor. Moreover, the input impedance increased with the Q factor, showing the characteristic of a parallel-type resonance. The calculated resonant frequencies (zero reactance) of the slot were 0.94 and 0.70 GHz for $\varepsilon_r = 3$ and 6, respectively, which agreed reasonably well with the predicted values of 1.0 and 0.77 GHz using $f_r = c/(2L\sqrt{\varepsilon_{\mathrm{re}}})$, where $\varepsilon_{\mathrm{re}} = (1 + \varepsilon_r)/2$ is the effective dielectric constant of the slot. For the cavity resonances, their resonant frequencies (minimum resistance) were predicted accurately using their eigenvalues.

V. Conclusion

A slot on a spherical cavity has been studied. The rigorous Green's functions interior and exterior to the cavity have been derived and the overall solution is very computationally efficient. The moment method has been used to find the unknown magnetic current in the slot. The techniques used in the planar slot have been modified and applied to the present curvilinear slot so that the problem of singularity in admittance calculations has been avoided. From the magnetic current, the input impedance of the structure has been found. Measurements were done to verify the theory, and very good agreement between theory and experiment has been obtained.

The slot and cavity resonances of the structure have been found and discussed. For the cavity resonance, both the natural and forced resonances have been addressed. The effects of the slot length, cavity size, excitation offset, and cavity dielectric constant on the input impedance have been studied. It has been found that when the slot length is small (or, equivalently, the cavity is large), a strong coupling between the slot and cavity resonances occurs. For the excitation offset, it can be used to change the impedance level. With the offset, the first harmonic of the slot has been also excited. To decrease the operating frequency, the cavity can be filled with dielectric material, at the expense of smaller bandwidth and reduced radiation.

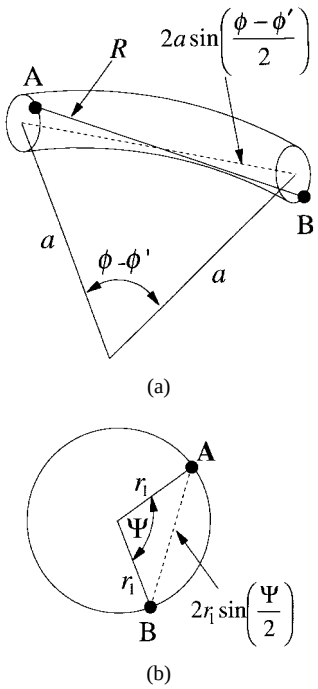

Fig. 7. The approximate distance R of (26) and the angle Ψ in the Appendix.

The theory and techniques presented in this paper are useful for other related problems. For example, based on the theory, the structure with a backing cavity for the slot can be easily analyzed.

Appendix

The exact expression of the distance between the field and source points is, in spherical coordinates, given by

$$R_{\mathrm{exact}} = \sqrt{r^2 + r'^2 - 2rr'\cos\xi} \tag{A1}$$

where $\cos\xi$ has been defined in (5). Unfortunately, this expression is not suitable for mathematical simplification. Instead, an approximate expression was used, which is given by [20]

$$R' = \sqrt{4a^2\sin^2\left(\frac{\phi-\phi'}{2}\right) + 4r_1^2\sin^2\left(\frac{\Psi}{2}\right)} \tag{A2}$$

where Ψ is an angle illustrated in Fig. 7. Note that $R' = 0$ when $\phi = \phi'$ and $\Psi = 0$, which causes a singularity in admittance calculations. To avoid the singularity, we have used the following approximation in deriving (24):

$$\frac{e^{-jkR}}{R} \approx \frac{1}{2\pi}\int_0^{2\pi}\frac{e^{-jkR'}}{R'}\,d\Psi \tag{A3}$$

where R has been defined in (26). Note that (A3) is analogous to the reduced kernel for a cylindrical dipole antenna [21].

Acknowledgment

The author would like to thank K. Y. Chow and K. K. Tse for their help in the measurement process. The valuable comments from Prof. T. K. Sarkar is gratefully appreciated.

REFERENCES

[1] P. R. Karr, "Radiation properties of spherical antennas as a function of the location of the driving force," *J. Res. Natl. Bur. Stand.*, vol. 46, pp. 422–436, 1951.

[2] Y. Mushiake and R. E. Webster, "Radiation characteristics with power gain for slots on a sphere," *IRE Trans. Antennas Propagat.*, vol. AP-5, pp. 47–55, Jan. 1957.

[3] V. V. Liepa and T. B. A. Senior, "Modification to the scattering behavior of a sphere by reactive loading," *Proc. IEEE*, pp. 1004–1011, Aug. 1965.

[4] C. C. Lin and K. M. Chen, "Improved radiation from a spherical antenna by overdense plasma coating," *IEEE Trans. Antennas Propagat.*, vol. AP-17, pp. 675–678, Sept. 1969.

[5] ———, "Radiation from a spherical antenna covered by a layer of lossy hot plasma," *Proc. Inst. Elect. Eng.*, vol. 118, pp. 36–42, Jan. 1971.

[6] S. J. Towaij and M. A. K. Hamid, "Diffraction by a multilayered dielectric-coated sphere with an azimuthal slot," *Proc. Inst. Elect. Eng.*, vol. 119, pp. 1209–1214, Sept. 1971.

[7] S.-H. Zhu, K.-M. Chen, and H.-R. Chuang, "Interaction of the near-zone fields of a slot on a conducting sphere with a spherical model of man," *IEEE Trans. Microwave Theory Tech.*, vol. MTT-32, pp. 784–795, Aug. 1984.

[8] M. A. Plonus, "Electromagnetic scattering by slots on a sphere," *Proc. Inst. Elect. Eng.*, vol. 115, pp. 622–626, May 1968.

[9] K. Inami, K. Sawaya, and Y. Mushiake, "Mutual coupling between rectangular slot antennas on a conducting concave spherical surface," *IEEE Trans. Antennas Propagat.*, vol. AP-30, pp. 927–933, Sept. 1982.

[10] D. M. Pozar, "Reciprocity method of analysis for printed slot and slot-coupled microstrip antenna," *IEEE Trans. Antennas Propagat.*, vol. AP-34, pp. 1439–1446, Dec. 1986.

[11] K. W. Leung, K. M. Luk, K. Y. A. Lai, and D. Lin, "Theory and experiment of a coaxial probe fed hemispherical dielectric resonator antenna," *IEEE Trans. Antennas Propagat.*, vol. 41, pp. 1390–1398, Oct. 1993.

[12] A. Hadidi and M. Hamid, "Analysis of Gaussian cavity-backed slot radiator," *Can. J. Phys.*, vol. 68, pp. 1138–1148, Oct. 1990.

[13] M. I. Hussein and M. Hamid, "Scattering by a perfectly conducting multislotted cylinder," *Can. J. Phys.*, vol. 70, pp. 55–61, Jan. 1992.

[14] K. W. Leung, K. M. Luk, K. Y. A. Lai, and D. Lin, "Theory and experiment of an aperture-coupled hemispherical dielectric resonator antenna," *IEEE Trans. Antennas Propagat.*, vol. 43, pp. 1192–1198, Nov 1995.

[15] R. F. Harrington, *Time Harmonic Electromagnetic Fields*. New York: McGraw-Hill, 1961.

[16] J. D. Kraus, *Antennas*, 2nd ed. New York: McGraw-Hill, 1988, pp. 391–392.

[17] S. A. Long, "Experimental study of the impedance of cavity-backed slot antennas," *IEEE Trans. Antennas Propagat.*, vol. AP-23, pp. 1–7, Jan. 1975.

[18] K. W. Leung and K. Y. Chow, "Theory and experiment of the hemispherical cavity-backed slot antenna," *IEEE Trans. Antennas Propagat.*, vol. 46, pp. 1234–1241, Aug. 1998.

[19] E. M. Biebl and G. L. Friedsam, "Cavity-backed aperture antennas with dielectric and magnetic overlay," *IEEE Trans. Antennas Propagat.*, vol. 43, pp. 1226–1232, Nov. 1995.

[20] R. W. P. King and G. S. Smith, *Antennas in Matter*. Cambridge, MA: MIT Press, 1981, ch. 9.

[21] R. S. Elliott, *Antenna Theory and Design*. Englewood Cliffs, NJ: Prentice-Hall, 1981, pp. 569–572.

Kwok Wa Leung (S'91–M'92) was born in Hong Kong, on April 11, 1967. He received the B.Sc. degree in electronics and the Ph.D. degree in electronic engineering from the Chinese University of Hong Kong, Kowloon, Hong Kong, in 1990 and 1993, respectively.

From 1990 to 1993, he was a Graduate Assistant in the Department of Electronic Engineering, Chinese University of Hong Kong. Since 1994, he has been an Assistant Professor in the Department of Electronic Engineering, City University of Hong Kong, Kowloon, Hong Kong. His research interests include dielectric resonator antennas, microstrip antennas, wire antennas, numerical methods in electromagnetics, and mobile communications.